A Parallel Power Conditioning System with Energy Storage Capability for Power Quality Improvement in Industrial Plants

Domenico Casadei, Gabriele Grandi, Claudio Rossi

DIPARTIMENTO DI INGEGNERIA ELETTRICA
Università degli Studi di Bologna
via Risorgimento, 2 I-40136 Bologna ITALY
email: claudio.rossi@mail.ing.unibo.it

Keywords: Active filters, Power conditioning, Power quality, SMES, Emerging topologies

Abstract

Power Conditioning System (PCS) with energy storage capability is proposed as a viable solution for improving the power quality in industrial plants. Several tasks, such as reactive power compensation, current harmonic reduction, and smoothing of pulsating loads can be performed at the same time. In this paper the principle of operation of the PCS will be described, and the analysis will be focused on the control of the energy flow among the system components. Numerical simulations and experimental tests will be shown to demonstrate the effectiveness of the PCS to reduce flicker phenomena and to compensate harmonic current components and reactive power. With minor changes of the hardware structure and of the control algorithms the PCS can also be operated as Uninterruptible Power Supply (UPS).

I. Introduction

In industrial applications some types of high power loads are required to be switched on and off with a period less than 0.5 s. During the switching on of these loads, the demanded high currents determine a voltage drop across the line impedance, which is responsible of flicker phenomena. The main task of the developed PCS is to reduce the negative effects of pulsating loads, besides to the compensation of reactive power and current harmonics of non linear loads. For this purpose a suitable PCS scheme, based on the transfer of energy between the network and the energy Storage Device (SD) is proposed. Two basic configurations for a PCS can be defined according to the type of energy storage device. The former is based on a Superconducting Magnet (SM), the latter is based on a Supercapacitor (SC) bank. The control system that manages the energy transfer is the same for both the energy storage devices, it is called Energy Control System (ECS) and it will be described in Section II.

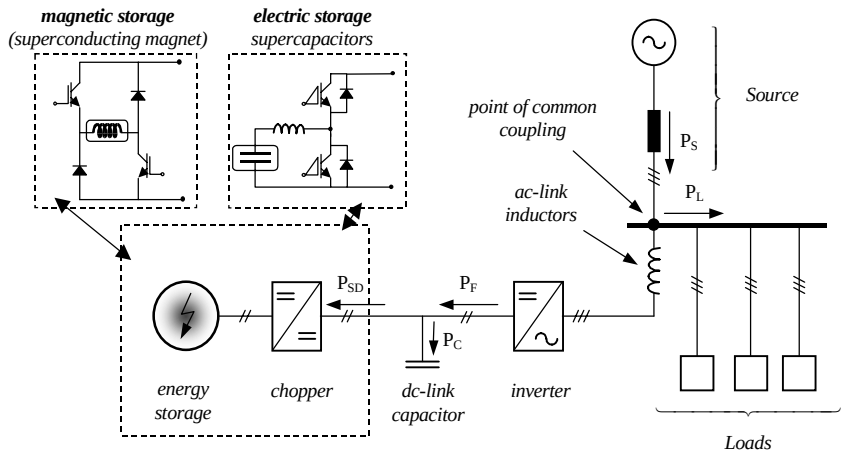

Fig. 1 Scheme of the PCS system

The scheme of the proposed PCS is shown in Fig. 1. The energy storage device is connected to a dc-dc converter allowing the bi-directional transfer of energy with the dc-link intermediate bus. The topology of the dc-dc chopper depends on the type of energy storage device.
Fig. 1 shows in detail the schemes required by SM and SC respectively. The dc-link bus is connected to the dc side of a three phase

Voltage Source Inverter (VSI), which is shunt connected to the mains through three ac-link inductors. The dc/ac section of the PCS has the same topology of a shunt active power filter [1]-[6].

The availability of an energy storage device allows the system to compensate the flicker phenomena introduced by pulsating loads. The active filter section of the PCS allows to compensate the reactive power, to reduce the load current harmonics and to eliminate the load current unbalance. The flicker compensation achieves the smoothing of the source power variations due to the switching on and off of the load [7]. During these transients the PCS operates in order to deliver the difference between the instantaneous load power and its average value.

The VSI is used to perform the direct control of the currents on the ac-link inductors. In this way the source currents are forced to follow the balanced and sinusoidal reference waveforms for any operating condition. The source currents are always synchronized with the fundamental positive sequence component of the source voltages. As a consequence, balanced and sinusoidal source currents with unity power factor are achieved, even in presence of voltage perturbations coming from the mains [8], [9]. The balanced and sinusoidal waveforms of the source currents are derived from the source power reference, which is generated by the ECS.

The capability of the proposed PCS to keep under control the source power flow for any operating condition is ensured by the use of a reliable synchronization device. The synchronization of the inverter output with the fundamental positive sequence component of the source voltages is carried out by means of a Three Phase Locked Loop (TPLL). This algorithm operates correctly even in presence of unbalanced and non sinusoidal voltages.

Numerical results and experimental tests showing the effectiveness of the PCS in terms of reduction of the harmonic currents of non linear loads, and smoothing of the source power due to pulsating loads will be presented.

II. Control System Analysis

Principle of operation

The combined operation of the PCS as active filter and flicker smoother is achieved by a suitable control algorithm, that manages the energy transfer among the energy storage device, the dc-link capacitor, and the mains.

The analysis of the ECS is based on the following assumptions:

- the control systems of the two converters are able to keep the source power P_S , and the storage device power P_{SD} close to their reference, i.e. P_S^* and P_{SD}^* ;
- losses in passive components such as inductors, capacitors, storage device, and in the static switches are neglected.

These two assumptions are acceptable because of the low time response of the control system used to drive the two converters and the small amount of the losses in the passive components. Furthermore, the time constant of the storage device must be low enough to allow the tracking of the energy variations demanded by the ECS.

The analysis of the ECS can be usefully carried out in terms of power flow and energy balance using the Laplacian notation [12], [13]. The proposed control algorithm is shown in the scheme of Fig.2. In this scheme the input control variables of the PCS are the energy in the dc-link capacitor E_C^*, and the energy in the storage device E_{SD}^*.

The regulator R_1 generates the reference source power, which combined to the load power gives the reference filter power. This last has to be injected by the inverter into the Point of Common Coupling (PCC). At the same time, the regulator R_2 generates the firing signals for the dc/dc chopper, which controls the power flowing into the storage device. The regulator $R_3(s)$ varies the energy reference in the SD on the basis of the error of the dc capacitor energy. Once the parameters of regulators R_1 R_2 and R_3 are defined, it is possible to determine the transfer functions of the control loops represented in Fig. 2.

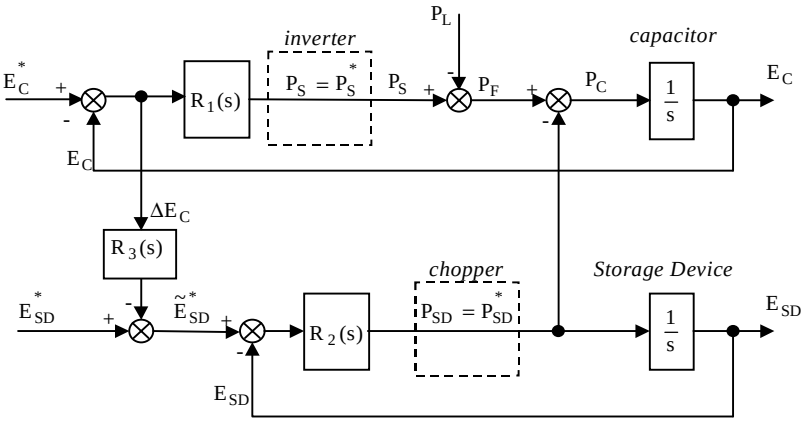

Fig. 2 - Energy Control System

The control algorithm has been designed to manage the transfer of energy between the SD and the dc-link capacitor during the transient conditions caused by load variations. In this way, the ECS operates in order to recover the energy level in the capacitor, using a fraction of the energy stored in the SD unit. During load changes, the energy variations in the capacitor are quickly compensated by the energy transfer between the SD and the dc-link capacitor. As a consequence, the energy required by the load can be considered as coming directly from the SD unit. The source is not required to supply the full load power, but an increasing amount of power. The use of the SD unit to smooth the load variations is necessary because the dc link capacitor has very few stored energy. Moreover, its energy variation must be minimized in order to ensure a correct operation of the inverter with a practically constant dc-link voltage.

Assuming the capacitor energy and the SD energy close to their references, respectively E_C^* and E_{SD}^*, an increase of the load power P_L determines a power flow from the capacitor to the ac side, yielding to an error $\Delta E_C = E_C^* - E_C$ in the capacitor stored energy. Assuming a simple proportional regulator the new SD energy reference will be given by:

$$\tilde{E}_{SD}^* = E_{SD}^* - K_{P3}\Delta E_C \ . \qquad (1)$$

This new lower value of the reference allows the chopper to recover the dc-link voltage using the energy stored in the SM or SC.

Numerical Analysis of the Energy Control System

Depending on the PCS feature which has to be analyzed, it is opportune to utilize different quantities has input and output variables of the ECS of Fig. 2. In [12] the analysis has been carried out with reference to the capability of the PCS to behave as active filter. Here the attention is focused to the possibility of the PCS to compensate the flicker phenomena due to pulsating loads. For this purpose, it is useful to consider the scheme shown in Fig. 3, which relates the source power P_S to the load power P_L.

Analyzing the transfer function of the control loop given in Fig. 3, it is possible to emphasize the PCS performance in smoothing the source power variations due to pulsating loads. The control scheme of Fig. 3 is derived from the basic scheme of Fig. 2, by considering the load power P_L as input signal, and the source power P_S as output variable. The references for the dc-link capacitor energy and for the SD energy, can be considered as disturbances having a constant value.

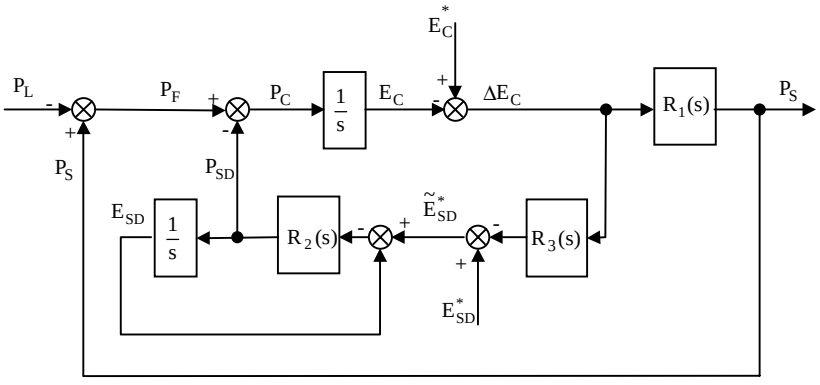

Fig. 3 - Block diagram showing the relationship between P_L and P_S

The relationship between the source power and the load

power can be easily calculated assuming for the regulators of Fig. 3 the following expressions:

capacitor energy regulator: $R_1(s) = K_{P1} + \frac{K_{I1}}{s}$

storage device energy regulator: $R_2(s) = K_{P2}$

SD energy reference regulator: $R_3(s) = K_{P3}$, with $K_{P3} >> 1$.

With these assumptions the expression for $P_S(s)$ is given by the sum of three terms as represented in (2) and in Fig. 4.

$$P_S(s) = G_C(s)E_C^* + G_{SD}(s)E_{SD}^* + G_L(s)P_L \qquad (2)$$

The expressions of $G_C(s)$, $G_{SD}(s)$, $G_L(s)$ are given in Appendix.

Under the assumption that E_C^* and E_{SD}^* are constant, by applying the final value theorem to the step response of the transfer functions $G_C(s)$, $G_{SD}(s)$ yields

$$\begin{cases} \lim_{s\to 0} s\frac{1}{s}G_C(s) = 0 \\ \lim_{s\to 0} s\frac{1}{s}G_{SD}(s) = 0 \end{cases} . \qquad (3)$$

This means that the relationship between the source power and the load power is given only by the transfer function $G_L(s)$. On the basis of this result, the analysis of the control system can be carried out with reference to the following open loop transfer function derived from $G_L(s)$,

$$G_{La}(s) = \frac{(K_{P1}s + K_{I1})(s + K_{P2})}{s^2(s + K_{P3}K_{P2})} . \qquad (4)$$

The resulting control system can be simplified as represented in Fig.5.

The parameters of the transfer function (4) must be tuned in order to obtain the desired behaviour of the source power in response to a load power variation.

The parameters K_{P1} and K_{I1} define the behavior of the regulator $R_1(s)$ in keeping constant the energy stored in the dc capacitor. The error in the capacitor energy determines directly the reference value of the power that the source has to supply. An integral action in the capacitor energy regulator is necessary in order to determine a small overshoot in the P_S behavior consequently to a step variation of P_L. The overshoot of P_S, with respect to the load power, is necessary to restore the energy level in the capacitor and in the storage device. The smaller is the overshoot the longer is the time necessary to recover the energy level in the SD and in the capacitor.

The parameter $K_{P2,}$ of the regulator $R_2(s)$, defines the performances of the system in following the quick changes of the reference level of $\tilde{E}_{SD}^*$. The higher is K_{P2}, the faster is the SD energy regulator. Using a suitable value for K_{P2}, the PCS determines a transient of the source power without discontinuities in response to a step variation of the load power.

The parameter K_{P3} defines the capability of the PCS to utilize the energy stored in SD. For a given load power variation, K_{P3} defines the corresponding energy reference variation in the SD and then the amplitude of the source power variation. With reference to a load switching on transient, the energy reference for the SD will be decreased of an amount related to the value of $K_{P3.}$ A deep discharge of the Storage Device determines a greater amount of energy flowing from the PCS towards the PCC,

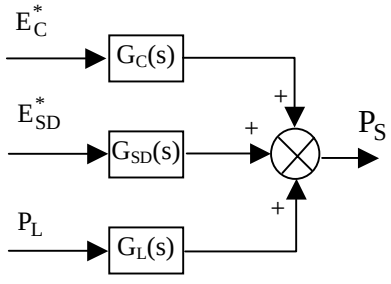

Fig. 4 Simplified block diagram of Eq. 2

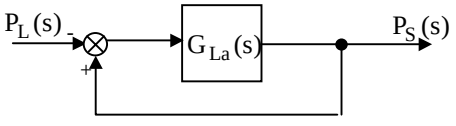

Fig. 5 Source power regulation loop

Table I – Main data of the PCS under analysis

SD energy reference	E^*_{SD}	150 [kJ]
dc capacitor energy reference	E^*_C	0.8 [kJ]
load power	P_L	30 [kW]

Table II - Regulator parameters of the Energy Control System

$R_1(s)$	K_{P1}	300
	K_{I1}	50
$R_2(s)$	K_{P2}	30
$R_3(s)$	K_{P3}	50

yielding to a longer time interval during which the PCS supplies the load power. The tuning of K_{P3} defines directly the capability of the PCS to smooth the load power variations, and then the capability of the PCS to reduce flicker phenomena introduced by load pulsations.

The performance of a PCS characterized by the data given in Tab. 1 has been analyzed. The SD energy is high enough to allow the supply of the load during short blackouts of the mains. As a consequence, during the operation of the system as power conditioner, the energy variations in the storage device are very small, and this is because the SD must retain enough energy to sustain the load for a given time period.

The tuning of the three regulators is carried out by numerical simulations of the control scheme of Fig. 3, using Matlab. Table II shows the regulator parameters of the analysed ECS. The control scheme of Fig. 3 has been also analysed to verify its stability. The transfer function $G_{La}(s)$ gives satisfactory results in terms of stability, being the phase margin always high.

III. Implemented Control System

The ECS described in the previous Sections has been implemented introducing some changes with respect to the basic scheme of Fig. 2.

The energy level in the dc-link capacitor is kept under control through the capacitor voltage V_C, and the source power through the source current $\bar{i}_S$ [6]. Figs. 6 and 7 show the control system modified with respect to the scheme of Fig.2, according to the previous considerations.

The reference source current $\bar{i}^*_S$ is obtained by multiplying the unity vector $\hat{e}^{+1}_S$, by the reference source current magnitude I^*_S, where:

- the unity vector $\hat{e}^{+1}_S$ is in phase with the positive sequence fundamental component of the line voltage $\bar{e}_S$, and it is generated by a proper Three Phase Locked Loop circuit.
- the reference source current magnitude I^*_S is generated by the regulator $R_1(s)$, which operates on the instantaneous error between the reference value V^*_C and the actual value V_C of the dc-link voltage.

Once the reference value of the source current is generated, it has to be synthesized by the ac current regulator. This regulator must operate in order to keep the source current $\bar{i}_S$ close to its reference value $\bar{i}^*_S$. As a first step, the reference filter current $\bar{i}^*_F$ must be determined since the VSI acts directly on the filter current $\bar{i}_F$.

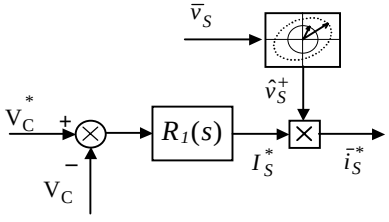

Fig. 6. dc-link voltage controller

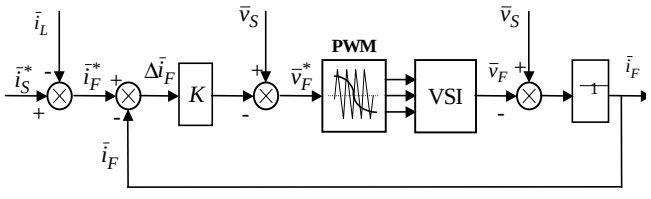

Fig. 7. ac current controller

The filter current is given by

$$\bar{i}_F^* = \bar{i}_S^* - \bar{i}_L , \qquad (5)$$

where the load current $\bar{i}_L$ is a measured quantity. The reference voltage $\bar{v}_F^*$ for the PWM-VSI can be generated by a regulator, using as input variable the difference between the reference and the actual value of the filter current

$$\Delta\bar{i}_F = \bar{i}_F^* - \bar{i}_F . \qquad (6)$$

The equation of the current controller can be expressed as follows

$$\bar{v}_F^* = \bar{v}_S - L_F \frac{\Delta\bar{i}_F}{\Delta t} = \bar{v}_S - K\Delta\bar{i}_F . \qquad (7)$$

This equation shows that the current controller behaves as a proportional controller having gain K, with an additional term for the source voltage compensation. On the basis of (5) and (7), the block diagram shown in Fig. 7 can be derived. It can be noted that the filter current is regulated through a closed loop control scheme.

Assuming that the VSI can generate the reference voltage at each cycle period, i.e. $\bar{v}_F = \bar{v}_F^*$, the following transfer function for the filter current can be obtained

$$\bar{i}_F = \frac{1}{1 + \frac{L_F}{K}s}\bar{i}_F^* . \qquad (8)$$

Eq. 8 shows that the response of the ac current controller is represented by a first order low-pass filter with a time constant $\tau = L_F/K$. The PCS behavior as active filter is mainly determined by the dynamic response of this current regulator.

Low values of L_F will determine fast current variations, and then a wide filter bandwidth. On the other hand, high values of L_F reduce the HF harmonics of the currents injected into the mains by the PCS, improving the voltage quality at the point of common coupling. According to (8), by increasing K it is possible to compensate high values of L_F. However, this possibility is limited by the maximum output voltage capability of the VSI, which is defined by the value of the dc-link voltage V_C.

The regulator $R_2(s)$ of the ECS, which is shown in the scheme of Fig.2, keeps under control the energy level in the storage device. In the implemented control system this has been achieved controlling the voltage across the supercapacitor, or the current flowing in Superconducting magnet. This regulation is performed by using a suitable PWM chopper, as it is shown in Fig.1.

In order to ensure the correct operation of the proposed PCS it is necessary to identify the source voltage system. The source voltage identification requires the on line calculation of the space vector corresponding to the positive sequence of the positive fundamental component $\left(\hat{e}_S^{+1}\right)$ of the source voltage. For this purpose an identification algorithm called Three Phase Locked Loop (TPLL) has been implemented [10], which is effective and reliable for every operating condition of the PCS, such as in the case of voltage unbalance or voltage distortion.

IV. Simulation and experimental results

Simulation results

The PCS, has been simulated by means of a model built in the Simulink environment of Matlab. This model represents accurately both the power scheme shown in Fig. 1, and the control scheme discussed in Section II. The control algorithm has been developed taking into account that in the experimental set up it will be implemented in a DSP board. For this reason the control system has been represented in the discrete time domain. Using this model the whole PCS has been tested in order to verify its capability to perform the several compensation tasks, which are expected from this

system. Numerical simulations have been carried out assuming as energy storage device a superconducting magnet, with a rated current of 150 A. Fig. 8 shows the response of the PCS during a load switching on.

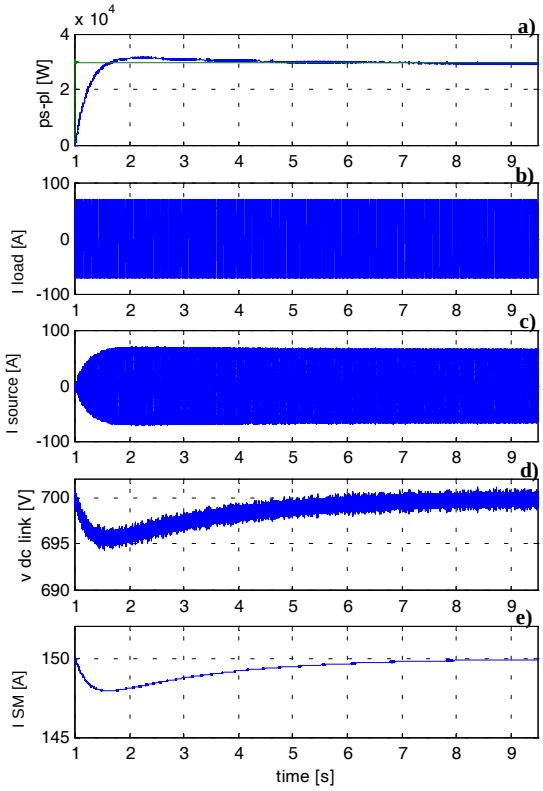

Fig. 8 Step response of the PCS to a load switching on. From top to bottom: a) source and load instantaneous power P_S-P_L; b) load curent; c) source current; d) dc link voltage V_C; e) magnet current I_{SM}

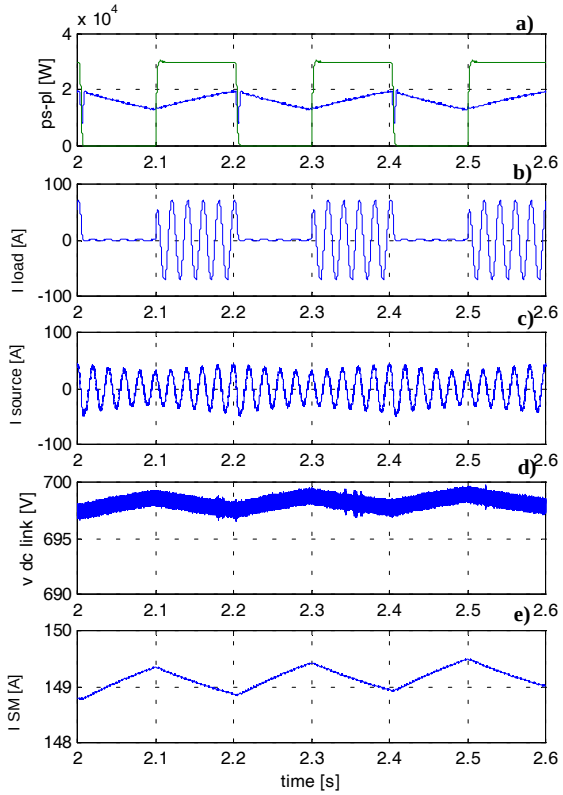

Fig. 9 Response of the PCS to a pulsating load. From top to bottom: a) source and load instantaneous power P_S-P_L; b) load curent; c) source current; d) dc link voltage V_C; e) magnet current I_{SM}

The results obtained are in agreement with the PCS performance, as expected on the basis of the analysis carried out in the previous Sections.

Experimental results

To validate the numerical simulations, a laboratory experimental set up has been assembled. The configuration of the experimental setup is exactly the same of that represented in Fig.1. The dc/dc converter, connecting the energy storage device with the dc-link, has the topology of a three phase inverter. In this way, the two dc/dc converter configurations shown in Fig. 1 can be easily implemented, depending on the type of device used to store energy.
At this stage of the project development, neither the Superconducting Magnet nor the Supercapacitor bank are available, then the operation of the proposed PCS as source power smoother has been tested using a flywheel driven by a three phase induction machine. The induction machine is controlled by the SD converter in its full configuration, i.e. a three phase inverter. The control algorithm of the SD inverter changes the speed of the flywheel to regulate the stored kinetic energy.

The control system has been digitally implemented on a PPC 333 MHz DSP based board. The board includes also the ADC converters and the encoder interface used to measure the rotating speed of the flywheel. By means of a PWM subsystem and an optoelectronic interface system, the firing signals for both the converters have been generated.
In this configuration the PCS, with the characteristics shown in Table III, is able to operate as smoother of load power variations and as active power filter. Fig. 10, 11, 12 emphasize the capability of this system to operate as active power filter. In particular, Fig. 10 shows the compensation of the

load reactive power, Fig. 11 the compensation of current harmonics due to non linear loads, Fig. 12 the compensation of a load unbalance due to a single phase load. Fig. 13, 14 show the behaviour of the PCS during the transient caused by a load switching on. The effects of the PCS is to smooth the corresponding step of the source power by supplying the load during the first instants of the transient.

This is achieved using a fraction of the energy stored in the flywheel. It can be noted that, after the first transient, the source power exceeds the load power of a small amount, necessary to restore the energy in the storage device at the reference value. At the end of the transient the source power equals

Table III – Main data of the experimental PCS

utility voltage	V_S	220 [V]	flywheel inertia	J_{SD}	0.3 [kg.m^2]
utility frequency	f_S	50 [Hz]	reference value of dc-link voltage	V_C^*	450 [V]
3 phase ac-link inductor	L_{ac}	2 [mH]	reference value of flywheel speed	ω_m^*	1250 [rpm]
dc-link capacitance	C_C	10 [mF]			

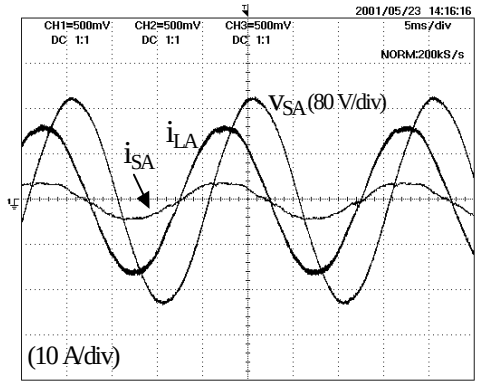

Fig. 10 Compensation of load reactive power

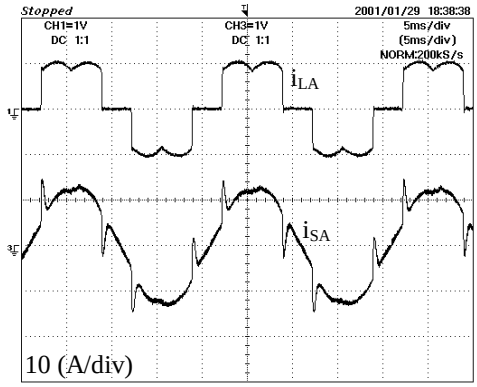

Fig. 11 Compensation of current harmonics

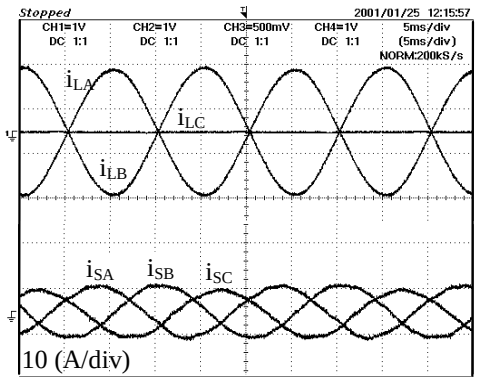

Fig. 12 Compensation of load unbalance

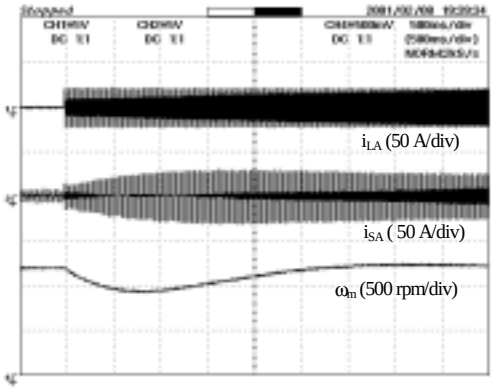

Fig. 13 Response of the PCS to a load switching on

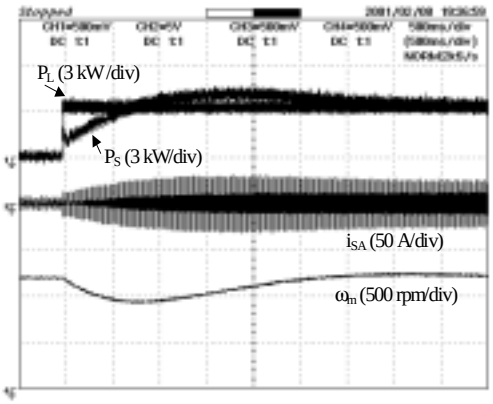

Fig. 14 Response of the PCS to a load switching on

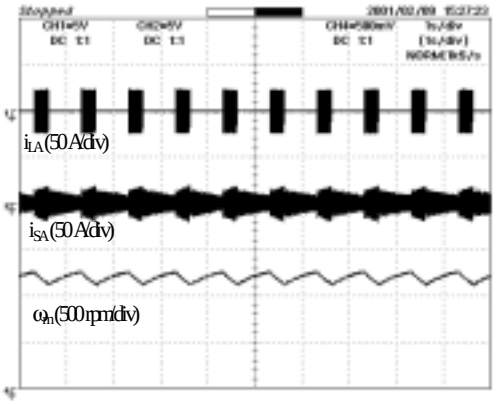

Fig. 15 Operation of the PCS with pulsating loads

the load power. Fig. 15 shows the behaviour of the system in the case of a pulsating load with a switching period of 1 second. The effect of the PCS is to keep the source current amplitude almost constant and equals to the mean value of the load active current. In the last three figures the load was very small (about 3 kW), so the weight of the losses in the induction machine and in the two converters are about 1/3 of the load power. Owing to this, the smoothing effect of the PCS is not much evident. Obviously increasing the load power will yield to better results.

V. Conclusion

A control scheme for Power Conditioning Systems, using different types of energy storage devices, has been analyzed in this paper.

The main feature of the proposed PCS is the possibility to meet several power quality requirements. This system is able to compensate reactive power and current harmonics due to linear or non-linear loads. The availability of energy stored in the SD gives the ability to compensate also the flicker phenomena. The configuration of the system allows further developments like the possibility to use the system as UPS during short time utility faults.

The control scheme has been numerically simulated in different operating conditions in order to set the parameters of the three regulators. A laboratory scale prototype has been realized at the university of Bologna. The experimental results are quite satisfactory, showing the effectiveness of the PCS in improving the power quality.

References

[1] L. Gyugyi, E.C. Strycula, "Active AC Power Filter," *Proc. IEEE-IAS Annual Meeting*, 1976, p. 529.

[2] H. Akagi, Y. Kanazawa, A. Nabae, "Instantaneous Reactive Power Compensators Comprising Switching Devices without Energy Storage Components," *IEEE Trans. on IA*, Vol. 20, 1984.

[3] L. Malesani, L. Rossetto, P. Tenti, "Active Filters for Reactive Power and Harmonic Compensation," *Proc. IEEE-PESC*, June 1986, p. 321.

[4] E. Raaijen et. al. "An Efficient and Economical Active AC Line Conditioner," *Proc. of IEEE-INTELEC*, The Hague, The Netherlands, Oct 29-Nov 1, 1995, pp. 664-670.

[5] L.A. Moran, J.W. Dixon, R.R. Wallace, "A three- phase active power filter operating with fixed switching frequency for reactive power and current harmonic compensation," *IEEE Trans. on IE*, Vol. 42, No.4, 1996, pp.402-408.

[6] D. Casadei, G. Grandi, U. Reggiani, C. Rossi, "Control methods for active power filters with minimum measurement requirements," *Proc. of IEEE-APEC*, Dallas-TX (USA), March 1999, Vol. 2, pp.1153-1158.

[7] D. Casadei, G. Grandi, U. Reggiani, G. Serra, "Analysis of a Power Conditioning System for Superconducting Magnetic Energy Storage", *IEEE-ISIE Conference*, Pretoria (SA), 7-10 July 1998, pp.546-551.

[8] D. Casadei, G. Grandi, U. Reggiani, G. Serra, A. Tani, "Behavior of a Power Conditioner for μ-SMES Systems under Unbalanced Supply Voltages and Unbalanced Loads," *Proc. of IEEE International Symposium on Industrial Electronics, ISIE*, Bled (SI), July 12-16, 1999.

[9] D. Casadei, G. Grandi, C. Rossi: "Effects of Supply Voltage non-Idealities on the Behavior of an Active Power Conditioner for Cogeneration Systems", *IEEE-PESC Conference*, Galway, Ireland, 18-23 June, 2000.

[10] F. M. Gardner, Phaselock Techniques. New York, Wiley 1979.

[11] S. K. Chung, "A Phase Tracking System for Three Phase Utility Interface Inverters", IEEE Transaction on Power Electronics, Vol. 15 no. 3, May 2000, pp.431-438

[12] D. Casadei, G. Grandi, U. Reggiani, C. Rossi, "Active AC Line Conditioner for a Cogeneration System" *European Confer. on Power Electronics and Applications, EPE*, Lausanne (CH), September 7-9, 1999.

[13] F. Negrini, U. Reggiani, C. Rossi, G. Grandi G. D. Casadei, et. al, "Recent Developments on micro-SMES System Project at the University of Bologna", *Proc. of EESAT*, Orlando-FL, USA, Sept. 17-20, 2000.

APPENDIX

With reference to the control scheme of Fig. 4, the expression of $G_C(s)$, $G_{SD}(s)$, $G_L(s)$are

$$G_C(s) = \frac{K_{P1}s^3 + (K_{P1}K_{P2} + K_{I1})s^2 + K_{P1}K_{P2}s}{s^3 + (K_{P1} + K_{P2} + K_{P3}K_{P2})s^2 + (K_{I1} + K_{P1}K_{P2})s + K_{P1}K_{P2}} \quad \text{(A1)}$$

$$G_{SD}(s) = \frac{K_{P1}K_{P2}s^2 + K_{PI}K_{P2}s}{s^3 + (K_{P1} + K_{P2} + K_{P3}K_{P2})s^2 + (K_{I1} + K_{P1}K_{P2})s + K_{I1}K_{P2}} \quad \text{(A2)}$$

$$G_L(s) = \frac{K_{P1}s^2 + (K_{P1}K_{P2} + K_{I1})s + K_{I1}K_{P2}}{s^3 + (K_{P1} + K_{P3}K_{P2})s^2 + (K_{I1} + K_{P1}K_{P2})s + K_{I1}K_{P2}}. \quad \text{(A3)}$$